Body Mass Index Effect on Ultrawideband MIMO BAN Channel Characterization

Seun Sangodoyin[†], *Student Member, IEEE*, Andreas F. Molisch[†], *Fellow, IEEE*
[†] University of Southern California, Dept. of Electrical Engineering, Los Angeles, CA 90089 USA
email:{sangodoy, molisch}@usc.edu

***Abstract*—This paper presents a detailed description of a measurement campaign for wireless Body Area Network (BAN) propagation channels in both an anechoic chamber and an indoor Lab environment. We use a self-developed 4 x 4 Ultrawideband (UWB) Multiple-input-multiple-output (MIMO) array channel sounding system operating in the 2 - 10 GHz frequency band. The main goal of the measurement is the determination of the impact of body mass index (BMI) on the on-body propagation channels. Using a total of 60 test subjects, we determine the BMI-dependence of channel paramaters such as pathloss (G_0), frequency-dependent decay factor (κ) and shadowing gain (χ_σ). We find that in particular, BAN channels of test subjects with BMI $>$ 30 show considerable difference to those of subjects with typical BMI.**

I. Introduction

Wireless Body Area Networks (BANs) have garnered a lot of attention over the years due to their potential for deployment in many fields ranging from wireless health care to surveillance and entertainment. Applications foreseen for BANs include vital sign detection [1], such as heart rate and blood pressure monitoring, which allows continuous care of patients as medical sensors on the body relay information to each other and/or a hub (e.g., a cellphone) that collects the information and forwards it from time to time to the medical staff. The preferred technology for implementing wireless BANs is ultrawideband (UWB) radio, due to qualities, such as low-power, high data rate, and robustness to fading [2]. UWB signals are defined as either having more than 20% relative bandwith or absolute bandwidth greater than 500 MHz [3] and are permitted to operate in the 3.1-10.6 GHz frequency band assigned by the Federal Communications Commission (FCC) in the USA. In addition to the use of UWB, recent suggestions for improving the BAN also includes the use of MIMO (multiple antennas at transmitter and receiver) to increase channel capacity.

Wireless system development requires a detailed characterization of the propagation channel in which the system will operate, hence it is of utmost importance that such a channel be characterized with consideration for factors such as frequency band of operation. Since narrowband and ultra-wideband channels are remarkably different [4], narrowband BAN models cannot be used for evaluation of UWB BANs, thereby necessitating a UWB BAN Model [5]. Furthermore, propagation of electromagnetic (EM) waves around the human body can be classified as either via surface waves or diffraction mechanism [2]. It is expected that the human body tissues will have a significant effect on the propagation especially when various body types (with different dimensions and tissue properties) are considered [6]. Tissue constituents of various human bodies differs remarkable. This implies that the BMI, which is a measure of human body fat based on height and weight [7] can be anticipated as a contributing factor in the characterization of EM waves around the body. For medical applications, modeling BAN propagation channels on people with very high BMI is particularly important, since it is exactly the people with very high BMI for whom medical BANs are especially relevant. However, previous measurements and models considered test subjects with BMI $<$ 25, yet the resulting channel models have been used for all BMI categories. Such a *one size fits all* approach is incomplete at best.

There have been a number of UWB BAN channel investigations based on measurements on a single person or a single phantom[1], e.g., [5], [8], and references therein. Furthermore, [9] analyzed the difference between propagation characteristics of three people with different weight. However, we are unaware of any measurement-based models which characterizes the UWB MIMO propagation channel responses based on the BMIs of a number of people sufficiently large to render results *statistically significant*.

In this paper, we describe a measurement campaign that employs a custom-designed 4 x 4 UWB MIMO array channel sounding system to perform BAN propagation channel measurements both in an anechoic chamber and indoor laboratory environments. We present results for key channel parameters such as average pathloss value (G_0), frequency-dependent decay factor (κ) and shadowing gain (χ_σ) with respect to different BMI categories.

The rest of this paper is organized as follows. Section II describes the measurement environment, while section III describes our measurement setup. Data processing procedure and results obtained are described in Section IV. Conclusions are drawn in Section V.

II. Measurement Environment

We conducted the measurements in the UltRa Lab facility located at the University of Southern California (USC) in Los Angeles, CA, USA. The experiments were in both an anechoic chamber and indoor lab environments, which are shown in

[1]synthetic material in the shape, and with similar dielectric characteristics, of a human

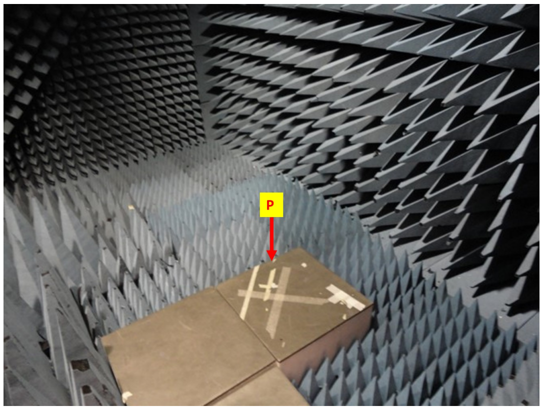

Fig. 1: Anechoic Chamber in the Ultralab at USC

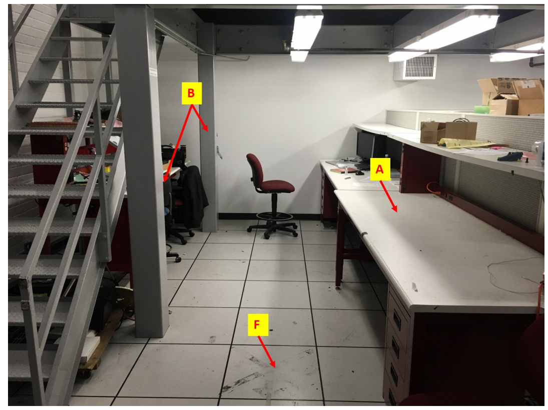

Fig. 2: Indoor Lab environment in the Ultralab at USC

Figs. 1 and 2 respectively. The anechoic chamber is a 9.1 x 4.6 x 4.6 m Radio Frequency (RF) shielded room, which serves as a controlled environment with little or no reflection while the indoor lab is a 13.1 x 15.2 x 6.0 m room mostly populated with metallic work benches, plastic chairs, computers and also houses the anechoic chamber. The ceiling, floor, and walls surrounding the indoor lab were made of reinforced concrete, with four metallic pillars serving as structural support for a mezzanine (also located in the lab) for storage of old equipment. The location of the actual experiment in the lab is a narrow aisle (as shown in Fig. 2) with exposure to a metallic workbench (labeled A), two metallic pillars (labeled B), a second work bench, boxes and a staircase leading to the aforementioned mezzanine. The human subject was positioned on a floor tile (labeled F).

In the anechoic chamber, three platforms were present with two serving as a walkway while the third served as the stand (labeled P) for the BAN subject. These positions and the structural composition of the environment was maintained for the duration of the entire measurement campaign.

TABLE I: Hardware used in the channel measurement

Item	Manufacturer	Model No.
VNA	Agilent	8720ET
TX/RX RF switch	Pulsar Microwave	SW8RD13
coaxial cables	RF Industries	RFW-5950-96
UWB antennas	XY	XY3

TABLE II: Measurement parameters

Parameter	Setting
Bandwidth	8 GHz (2 - 10 GHz)
Center frequency, f_c	6 GHz
Total number of Channels	16
Number of sub-carriers	801
delay resolution	0.125 ns
Frequency resolution	9.98 MHz

III. Measurement setup

The channel sounder system setup developed for our measurement campaign is shown in Fig. 3. The measurements were performed in the frequency domain using a vector network analyzer (VNA, Agilent 8720ET), which is used for obtaining the complex channel transfer function of the propagation channel. The VNA was calibrated along with two 2.7 m long coaxial cables at transmitter (TX) and receiver (RX) ends. This calibration was implemented from the antenna feed points of the coaxial cables, while a stepped frequency sweep was conducted for 801 frequency points within a range of 2-10 GHz. We employed a 4-element switched uniform linear antenna (ULA) array configuration at both the TX and RX ends using an in-house developed XY3 omni-directional antennas[10]. The antennas were placed 7.5 cm apart in the linear array configuration in most instances while switching between array elements was performed by Pulsar Microwave (SW8RD13) RF switches, with switching time of 100 ns and insertion loss of 3.5 dB. The RF Switches were calibrated separately with their system response subtracted from channel sounder response. The antennas are interpreted as part of the propagation channel. This is necessary because the presence of large dielectric objects (the human body) throughout the relevant propagation channel prevents the extraction of the usual double-directional channel representation [11].

Labview software was used to activate/deactivate a control circuit for the RF switches hence automating the channel measurement procedure. This software was also responsible for handling the data acquisition from the VNA. The test subjects wore a harness on the body to avoid the antenna directly contacting the body surface. Such contact would cause degradation in performance of the antenna and significantly influence the pathloss, hence this needed to be carefully controlled lest it lead to undesired random fluctuations of the results. In all cases, the antennas were mounted so they can be vertically polarized - parallel to the body surface - and kept at 0.95 cm from the body. A list of all equipment is given in Table I while all parameter settings for the channel measurement are shown in Table II.

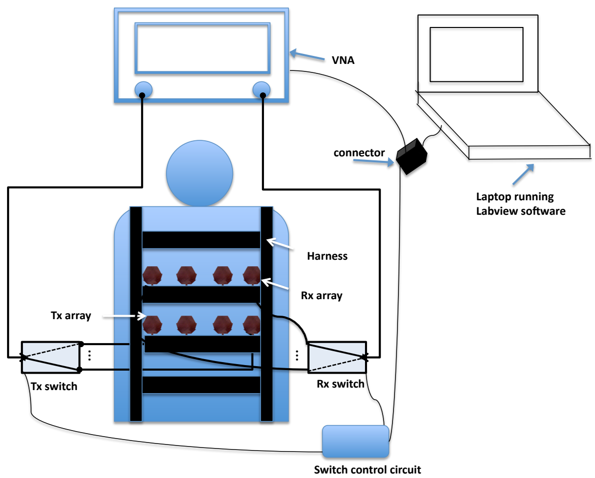

Fig. 3: UWB BAN Measurement setup with harness on the body

Different on-body channels were considered in our campaign, some of the channels measured are listed in Table IV (others can be found in [12]), while antenna placements for these channels are illustrated in Figs. 4(a), 4(b) and 5. We measured 60 male subjects with ages 18 years or older with various BMIs in work. We could not conduct experiments with female subjects since no female research personnel qualified to work on this Instititional Review Board (IRB)-approved project was available to work with female test subjects. The male test subjects were categorized according to their BMI values following a conventional medical classification [13], [14] as shown in Table III. The recruited subjects were later grouped such that there were 20 candidates *per* BMI category.

TABLE III: International Classification according to BMI

Category	BMI Value	Classification
1	18.5 - 24.9	normal
2	25 - 29.5	overweight
3	$\geq$ 30	obese

TABLE IV: Channels measured on the body

Channel	Location
1	Front-to-Front (F2F)
2	Front-to-Hip (F2H)
3	Front-to-back (F2B)

A key assumption for our measurement is that the channel is *static*, which is fulfilled if there are no posture variations/ movements from the human subject or moving scatterers in the environmental. We made sure there were no moving scatterers in the vicinity of our measurement setup, and also monitored and instructed all test subjects to keep still while the measurements were being conducted.

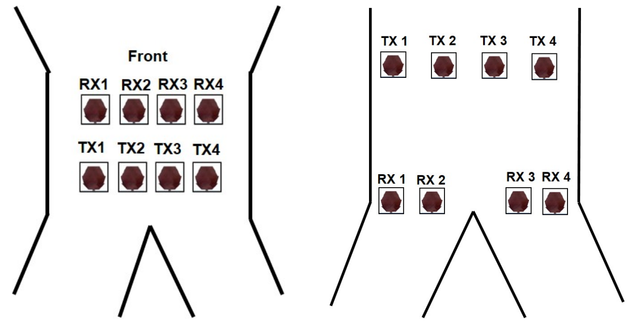

(a) (b)

Fig. 4: (a) F2F (b) F2H

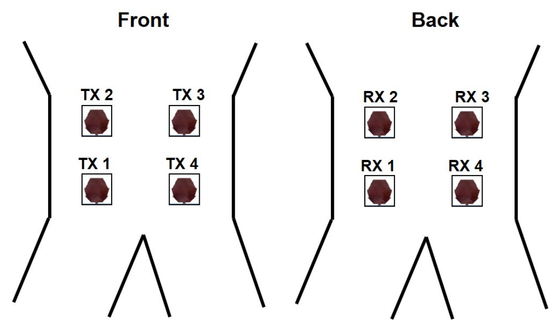

Fig. 5: F2B

IV. Data Processing and Results

The data acquired from the VNA are processed in order to extract the channel transfer function. The transfer function of each on-body channel measured is denoted as $H_{i,j,k,z,q,\psi,\xi}$, where $i \in [1,2,...,I = 4]$ and $j \in [1,2,...,J = 4]$ represent the TX and RX antenna position indices within the array, $k \in [1,2,...,K = 801]$ denotes the frequency points, $z \in [1,2,...,Z = 7]$ is the on-body channels measured, $q \in [1,2,...,Q = 20]$ represents the index of people per BMI category, $\psi \in [1,2,...\Psi = 3]$ indicates the BMI category index, and $\xi \in [1,...,\Xi = 2]$ represents the environments with $\xi = 1$ as the anechoic chamber and $\xi = 2$ as indoor lab environment, respectively. The transfer function $H_{i,j,k,z,q,\psi,\xi}$ was transformed to the delay domain by using an inverse Fourier transform and a Hanning window (to reduce side-lobes). The resulting impulse response is denoted as $h_{i,j,n,z,q,\psi,\xi}$, using similar index parameters representation as those of the transfer function with the exception of the frequency bin index changed to $n \in [1,2,...,N = 801]$, where n indicates the delay bin index.

$$\hat{P}_{n,z,q,\psi,\xi} = \frac{1}{I}\frac{1}{J}\sum_{i=1}^{I}\sum_{j=1}^{J} P_{i,j,n,z,q,\psi,\xi} \quad (1)$$

Using the impulse responses, we computed an instantaneous power-delay profiles (PDP) by taking the magnitude squared ($P_{i,j,n,z,q,\psi,\xi} = |h_{i,j,n,z,q,\psi,\xi}|^2$) of the impulse response. The influence of small-scale fading is reduced by averaging the PDP over all MIMO channels measured so as to obtain the average power-delay-profile (APDP) as shown in (1). Sample APDP plots obtained from some of the channels in the BMI categories for an indoor lab measurement are shown in Figs. 6(a) & 6(b) below.

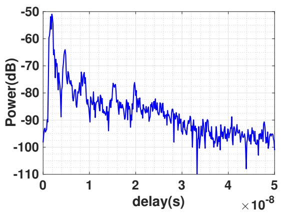

(a) APDP of F2F Channel

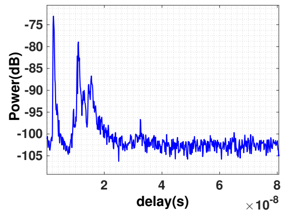

(b) APDP of F2B Channel

Fig. 6: APDP from sample measured channels in the indoor lab environment

A noise thresholding filter, which sets all APDP samples whose magnitudes are below a certain threshold to zero was implemented in our work. The threshold value is chosen to be 6dB above the noise floor of the APDP, while a delay-gating filter was implemented for anechoic chamber measurements, which eliminated MPCs in excess of a 4 m. The value 4 m was chosen because there were no observable reflector/scatterer that could cause a MPC with such a large excess runlength in the on-body channels.

A. Pathloss Analysis

According to [15], pathloss in the UWB channel exhibits both distance and frequency dependencies. A consequence of the nature of our work is that there are no distance dependencies on pathloss since each channel was measured at a fixed TX-RX separation. To this end we express the pathloss in the channel as:

$$\mathrm{G}_L(f, d_0) = \mathrm{G}_0 \cdot \mathrm{X}_\sigma \cdot \mathrm{G}_L(f) \tag{2}$$

where G_0, X_σ and $\mathrm{G}_L(f)$ are the average pathloss at a fixed distance ($d = d_0$) , shadowing gain and the frequency-dependent pathloss (to be discussed subsequently) respectively. For each test subject, we compute the local mean power ($\mathrm{M}_0^{z,q,\psi,\xi}$) as shown in (3))

$$\mathrm{M}_0^{z,q,\psi,\xi} = \sum_{n=1}^{N} \hat{P}_{n,z,q,\psi,\xi} \tag{3}$$

from which we can then compute G_0 as

$$\mathrm{G}_0^{z,\psi,\xi} = \frac{1}{Q} \sum_{q=1}^{Q} \mathrm{M}_0^{z,q,\psi,\xi} \tag{4}$$

Values for G_0 obtained from our measurements are provided in Table V. Cumulative distribution function (CDF) plots for M_0 in different BMI categories and environments for channel F2H are shown in Figs. 7(a) and 7(b).

It can be observed from the values of G_0 in Table V that the pathloss values do differ for various BMI categories in both environments measured. The differences between categories BMI 1 and 2 are mostly around 2 dB; however the pathloss for BMI 3 shows a significant increase compared to other categories, namely from 3 to 13 dB. This confirms an intuitive assumption that there would be a higher pathloss in BMI 3 since anatomically, there is more body mass to transverse and exposure to more body tissue, which will likely attenuate the transmitted signal.

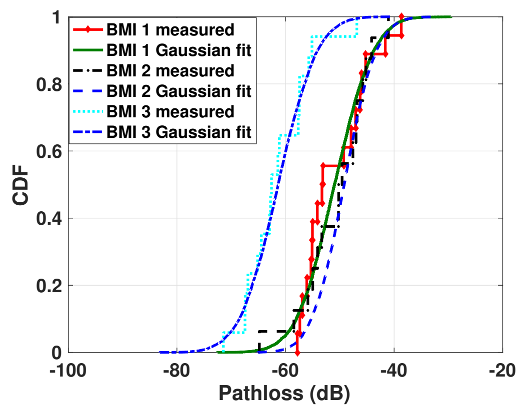

(a) CDF of pathloss for F2H in an Anechoic chamber

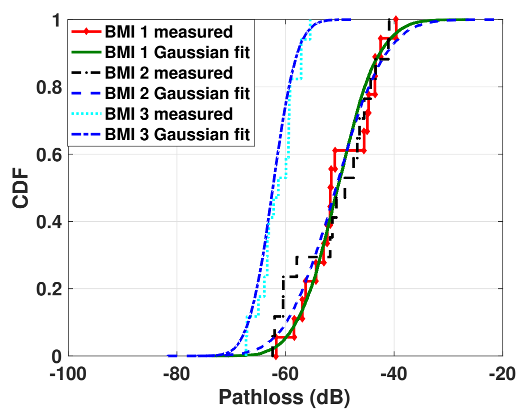

(b) CDF of pathloss for F2H in an Indoor Lab

Fig. 7: CDF of Pathloss for F2H channel

The frequency dependence of the pathloss arises primarily from the antenna power density and gain variation, the tissue constituents of the human body, and the physical propagation phenomena such as scattering and diffraction in the channel. The frequency-dependent pathloss , $\mathrm{G}_L(f)$, is expressed as an expansion of a power-law decay model [15]

$$\mathrm{G}_L(f) = \zeta \left(\frac{f}{f_0}\right)^{2\kappa} \tag{5}$$

where κ is the frequency decay factor, ζ is a normalization constant, f_0 is the center frequency and each sub-band is 500 MHz. The value of κ extracted for various on-body channels are provided in Table V. Again we observe a significant increase for some channels in BMI 3.

B. Shadowing

The shadowing gain (X_σ) accounts for the fluctuations of the received power in different on-body channels with respect to the BMI category in which the experiment is being conducted. The shadowing gain was obtained by subtracting the mean pathloss from the pathloss of all human subjects in a particular BMI category and environment. The logarithmic values of the shadowing gain was found to follow a zero-mean Gaussian distribution. A sample distribution plot for the F2F channel in BMI category 1 for both environments measured is shown in Fig. 8 below. Standard deviation (std. dev) values for all channels and BMI categories measured in the Anechoic and Indoor environments are shown in Table V.

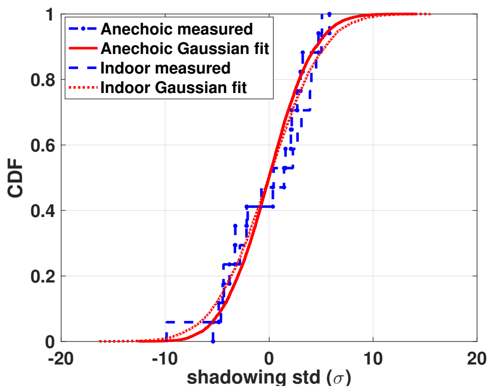

Fig. 8: CDF of shadowing gain for F2F channel in BMI 1

TABLE V: Parameters extracted for various channels and BMI categories

Average Pathloss, G_0 (dB)						
	F2F		F2B		F2H	
	Anec.	Ind.	Anec.	Ind.	Anec.	Ind
BMI 1	-39.40	-40.78	-72.68	-63.62	-49.23	-50.69
BMI 2	-41.91	-41.66	-72.17	-65.98	-50.90	-50.18
BMI 3	-47.55	-45.76	-86.37	-74.57	-63.58	-63.58
Frequency-dependent decay factor (κ)						
BMI 1	1.05	1.06	1.21	1.22	1.20	1.22
BMI 2	1.04	1.05	1.31	1.36	1.21	1.21
BMI 3	1.04	1.13	1.86	1.57	1.46	1.43
Shadowing gain, σ_s(dB)						
BMI 1	2.69	4.55	8.57	6.65	5.88	7.12
BMI 2	3.50	4.21	5.54	3.77	5.61	6.06
BMI 3	4.27	2.55	2.90	5.88	5.22	3.54

V. Conclusion

We devised a UWB MIMO measurement setup, and performed an extensive measurement campaign to understand the impact that BMI has on propagation channel parameters. We found the pathloss to vary significantly among the BMI categories (even up to 13 dB) in BMI 3 case. Frequency-decay factor κ values, were slightly higher in BMI 3 in some cases as well. We found the shadowing gain to vary from 2.55 to 8.57 dB for channels measured. These results validates our assumption that a *one size fits all* approach to channel measurement and modeling is inadequate and that BAN modeling should be done with respect to various BMIs. The results can be used for system design and link budgets for UWB BAN.

VI. Acknowledgment

The authors would like to thank Prof. Fredrik Tufvesson from Lund University, Sweden, for providing antennas used for earlier version of the experiment. They would also like to thanks Phil Philip for helping with the preliminary measurement setup, Dr. S. Niranjayan for helping with circuit design. Finally, the authors would like to thank the USC institution review board (IRB) for granting the permission to conduct the experiment.

References

[1] E. Jovanov and A. Milenkovic, "Body area networks for ubiquitous healthcare applications: Opportunities and challenges," *J Med Syst*, vol. 35, pp. 1245–1254, Oct. 2011.

[2] S.V.Roy, et al., "Propagation modeling for uwb body area networks: Power decay and multi-sensor correlations," in *10th International Symposium on Spread Spectrum Techniques and Applications*, Bologna, Italy, Aug. 2008, pp. 649–653.

[3] M. Di Benedetto and G. Giancola, *Understanding Ultra Wide Band Radio Fundamentals*, ser. Prentice Hall communications engineering and emerging technologies series. Pearson Education, 2004.

[4] A. F. Molisch, "Ultrawideband propagation channels-theory, measurement, and modeling," *IEEE Transactions on Vehicular Technology*, vol. 54, pp. 1528–1545, Sep. 2005.

[5] A. Fort, P. Doncker, and L. V. Biesen, "An ultra-wideband body area propagation channel model- from statistics to implementation," *IEEE Transactions on Microwave Theory and Techniques*, vol. 54, pp. 1820–1826, Apr 2006.

[6] Q. H. Abbasi, et al, "Numerical characterization and modeling of subject-specific ultrawideband body-centric radio channels and systems for healthcare applications," *IEEE Transactions on Information Technology in Biomedicine*, vol. 16, pp. 221–227, Mar. 2012.

[7] A. Keys, F. Fidanza, M. J. Karvonen, N. Kimura, and H. L. Taylor, "Indices of relative weight and obesity," *Journal of Chronic Diseases*, vol. 25, no. 6, pp. 329 – 343, 1972.

[8] S. L. Cotton, R. D'Errico, and C. Oestges, "A review of radio channel models for body centric communications," *Radio Science*, vol. 49, no. 6, pp. 371–388, 2014.

[9] X. Chen, X. Lu, D. Jin, L. Su, and L. Zeng, "Channel modeling of uwb-based wireless body area networks," in *IEEE International Conference on Communications*, vol. 6, 2011, pp. 1–9.

[10] X. S. Yang, J. Salmi, A. F. Molisch, S. G. Qiu, S. Sangodoyin, and B. Z. Wang, "Trapezoidal monopole antenna and array for uwb-mimo applications," in *2012 International Conference on Microwave and Millimeter Wave Technology (ICMMT)*, vol. 1, May 2012, pp. 1–4.

[11] M. Steinbauer, A. F. Molisch, and E. Bonek, "The double-directional radio channel," *IEEE Antennas and Propagation Magazine*, vol. 43, no. 4, pp. 51–63, Aug 2001.

[12] S. Sangodoyin and A. F. Molisch, "Impact of Body Mass Index on Ultrawideband MIMO BAN Channels - Measurements and Statistical Model," *to be submitted*.

[13] World Health Organization, "BMI Classification." [Online]. Available: http://apps.who.int/bmi/index.jsp?introPage=intro_3.html

[14] Centers for Disease Control and Prevention (CDC), "About Adult BMI." [Online]. Available: https://www.cdc.gov/healthyweight/assessing/bmi/adult_bmi/

[15] A. Molisch and et al., "A comprehensive standardized model for ultrawideband propagation channels," *IEEE Trans. Antennas Propag.*, vol. 54, pp. 3151–3166, Nov 2006.